SANDIA REPORT

SAND2015-10472
Unlimited Release
Printed December 2015

Peridynamic Multiscale Finite Element Methods

Timothy Costa, Stephen Bond, David Littlewood, Stan Moore

Prepared by
Sandia National Laboratories
Albuquerque, New Mexico 87185 and Livermore, California 94550

Sandia National Laboratories is a multi-program laboratory managed and operated by Sandia Corporation, a wholly owned subsidiary of Lockheed Martin Corporation, for the U.S. Department of Energy's National Nuclear Security Administration under contract DE-AC04-94AL85000.

Sandia National Laboratories

Issued by Sandia National Laboratories, operated for the United States Department of Energy by Sandia Corporation.

Available to DOE and DOE contractors from
U.S. Department of Energy
Office of Scientific and Technical Information
P.O. Box 62
Oak Ridge, TN 37831

Telephone: (865) 576-8401
Facsimile: (865) 576-5728
E-Mail: reports@adonis.osti.gov
Online ordering: http://www.osti.gov/bridge

Available to the public from
U.S. Department of Commerce
National Technical Information Service
5285 Port Royal Rd
Springfield, VA 22161

Telephone: (800) 553-6847
Facsimile: (703) 605-6900
E-Mail: orders@ntis.fedworld.gov
Online ordering: http://www.ntis.gov/help/ordermethods.asp?loc=7-4-0#online

SAND2015-10472
Unlimited Release
Printed December 2015

Peridynamic Multiscale Finite Element Methods

Timothy Costa
Department of Mathematics
Oregon State University
Corvallis, OR
costat@math.oregonstate.edu

Stephen Bond
Center for Computing Research
Sandia National Laboratories
Albuquerque, NM
sdbond@sandia.gov

David Littlewood
Center for Computing Research
Sandia National Laboratories
Albuquerque, NM
djlittl@sandia.gov

Stan Moore
Center for Computing Research
Sandia National Laboratories
Albuquerque, NM
stamoor@sandia.gov

Abstract

The problem of computing quantum-accurate design-scale solutions to mechanics problems is rich with applications and serves as the background to modern multiscale science research. The problem can be broken into component problems comprised of communicating across adjacent scales, which when strung together create a pipeline for information to travel from quantum scales to design scales. Traditionally, this involves connections between a) quantum electronic structure calculations and molecular dynamics and between b) molecular dynamics and local partial differential equation models at the design scale. The second step, b), is particularly challenging since the appropriate scales of molecular dynamic and local partial differential equation models do not overlap. The peridynamic model for continuum mechanics provides an advantage in this endeavor, as the basic equations of peridynamics are valid at a wide range of scales limiting from the classical partial differential equation models valid at the design scale to the scale of molecular dynamics. In this work we focus on the development of multiscale finite element methods for the peridynamic model, in an effort to create a mathematically consistent channel for microscale information to travel from the upper limits of the molecular dynamics scale to the design scale. In particular, we first develop a Nonlocal Multiscale Finite Element Method which solves the peridynamic model at multiple scales to include microscale information at the coarse-scale. We then consider a method that solves a fine-scale peridynamic model to build element-support basis functions for a coarse-scale local partial differential equation model, called the Mixed Locality Multiscale Finite Element Method. Given decades of research and development into finite element codes for the local partial differential equation models of continuum mechanics there is a strong desire to couple local and nonlocal models to leverage the speed and state of the art of local models with the flexibility and accuracy of the nonlocal peridynamic model. In the mixed locality method this coupling occurs across scales, so that the nonlocal model can be used to communicate material heterogeneity at scales inappropriate to local partial differential equation models. Additionally, the computational burden of the weak form of the peridynamic model is reduced dramatically by only requiring that the model be solved on local patches of the simulation domain which may be computed in parallel, taking advantage of the heterogeneous nature of next generation computing platforms. Additionally, we present a novel Galerkin framework, the 'Ambulant Galerkin Method', which represents a first step towards a unified mathematical analysis of local and nonlocal multiscale finite element methods, and whose future extension will allow the analysis of multiscale finite element methods that mix models across scales under certain assumptions of the consistency of those models.

Acknowledgments

This work was funded by the Physics and Engineering Models and Advanced Technology Development and Mitigation elements of the United States Department of Energy's Advanced Simulation and Computing (ASC) program under the management direction of Eliot Fang and Veena Tikare. The authors are thankful for insightful discussions with Stewart Silling, Ann Wills, and Nicolas Morales.

This page intentionally left blank.

Contents

Chapter 1

Introduction

The problem of computing quantum accurate, design-scale solutions to mechanics problems is rich with applications and serves as the background to modern multiscale science research. The problem can be broken into several components, that, if strung together correctly would include quantum phenomena at the continuum scale. These pieces are themselves connections between models that are valid at various scales. For example, in recent work [41] Thompson et al. develop the Spectral Neighbor Analysis Potential (SNAP), which trains interatomic potentials for molecular dynamics (MD) simulations from Density Functional Theory (DFT) simulations, thereby achieving quantum accurate simulations at the scale of molecular dynamics. In [22] Lehoucq and Silling described a method for calibrating the peridynamic model for continuum mechanics from molecular dynamics simulations. In this work we focus on continuing this chain of upscaled parameterizations through the development of multiscale finite element methods for peridynamic models of continuum mechanics and mixed local and nonlocal models.

In some sense the multiscale methods field is a direct nod to the limitations of scientific computing power. With unlimited resources, in many applications one would simply solve the finest scale to obtain the most accurate solution. Methods that adaptively track features do so to avoid resolving the entire domain to the level required near the feature. Methods that compute effective upscaled parameters typically do so because the fine-scale model is intractable, and so accuracy is traded for feasibility. However, as computing platforms evolve, methods should be prepared to take advantage of increased capabilities. In the context of next generation computing platforms (NGP) it is clear already that there is a generalization of the 'node' to include heterogeneous architectures such as GPGPU and Xeon Phi Coprocessor accelerators. In this environment, it is natural to ask that methods scale with node strength as well as with number of nodes. The Multiscale Finite Element Method (MSFEM) is well suited to answer this call. In the MSFEM [15], one first discretizes the domain into a collection of coarse elements. On each of these elements, independent decoupled microscale problems are solved to produce multiscale basis functions which are used in a global coarse simulation. Thus, as node strength increases local refinements increase accuracy, while as node number increases global refinement increases accuracy.

The peridynamic theory of solid mechanics, originally introduced by S. Silling in 2000, [1, 33, 34, 35, 36, 32, 39], is a nonlocal model that presents an advantage in multiscale modeling, as the basic peridynamic equations are valid at considerably shorter length scales than traditional partial differential equation models. In fact, through the use of generalized functions one can recover the molecular dynamic model directly from the peridynamic model. From the perspective of numerical

analysis this is a tremendous advantage, as it provides a unified mathematical framework for the analysis of multiscale methods for peridynamic models. Various aspects of multiscale modeling with peridynamics have been investigated in [2, 3, 21, 22, 25, 26, 29, 37, 38].

Finite element methods for peridynamic models have been under active investigation for several years [10, 11, 13, 14, 42, 43]. However, to the best of the authors' knowledge, no work on a multiscale finite element method has appeared. In this work we remedy that situation and present the first efforts toward a nonlocal multiscale finite element method, as well as a mixed locality method. The rest of these notes are organized as follows.

In Section 2 we present an abstract Galerkin framework we call the 'Ambulant Galerkin Method' (AGM). This method represents a first step towards a unified framework for the analysis of nonlocal and local multiscale finite element methods, as well as a framework for analyzing a more general multiscale infrastructure based on the computation of improved basis functions. In Section 3 we introduce the peridynamic model of solid mechanics. In Section 4 we go from the AGM framework to a nonlocal multiscale finite element method (Nl-MSFEM) for the peridynamic model. Additionally, we present a mixed-locality finite element method (ML-MSFEM) that couples nonlocal and local models for continuum mechanics. In Section 5 we present numerical experiments of the nonlocal multiscale finite element method and the mixed locality multiscale finite element method. Finally in Section 6 we give concluding remarks.

Chapter 2

Ambulant Galerkin Method

In this section we present a Galerkin framework called the 'Ambulant Galerkin Method' (AGM). This method is motivated by a desire for an abstract framework for the analysis of multiscale finite element methods designed for local, nonlocal, or mixed-locality problems. In particular, we obtain convergence results for Ambulant Galerkin methods, which represent an abstraction of multiscale finite element methods. We then identify the error induced by deriving multiscale finite element methods from the Ambulant Galerkin framework. Ultimately we are interested in a framework for the analysis of 'mixed' multiscale finite element methods, which couple varying models across scales. In future work we will combine the Ambulant Galerkin analysis here with the asymptotic compatibility framework of Tian and Du [42] to achieve that goal. The principal idea behind the method is the construction of a correction operator which translates an approximating subspace toward the true solution in order to reduce error without increasing the dimension of the approximating subspace. This section relies on some knowledge of functional analysis and Hilbert space methods [8, 31].

Let V be a Hilbert space, and $V' = \mathscr{L}(V,\mathbb{R})$ be the space of continuous linear functionals on V. Let $\mathscr{B} \in \mathscr{L}(V,V')$ be V-coercive and $f \in V'$. We consider the abstract problem

$$\text{find } u \in V \text{ s.t. } \mathscr{B}u - f \in V^o. \tag{2.1}$$

Here the superscript o denotes the annihilator of the space V,

$$V^o := \{f \in V' \,:\, f(v) = 0,\ \forall v \in V\}. \tag{2.2}$$

Our first step is to define an approximation space. Presumably this space has a low number of degrees of freedom, and produces an insufficiently accurate solution with standard methods. Let $V^H \subset V$ be a finite dimensional subspace with basis $\{\phi_i\}_{i=1}^{N_H}$, called the 'approximation space', and let $I^H : V \to V^H$ be an orthogonal projection operator.

In order to decompose the space V into a direct sum decomposition of V^H and a remainder space we take advantage of the properties of an orthogonal projection operator. Define the 'remainder space' V^r by

$$V^r = \{v \in V \,:\, I^H(v) = 0\}, \tag{2.3}$$

so that

$$V = V^H \oplus V^r. \tag{2.4}$$

Our goal now is to enhance the space V^H without increasing the total degrees of freedom in the approximation problem, i.e. without increasing the dimension of the approximation space V^H. To do this, we will define a correction operator that takes advantage of the direct sum decomposition $V = V^H \oplus V^r$ to translate the space V^H within V to a space of the same dimension, which contains the exact solution. This correction operator $Q : V^H \to V^r$ is defined as the solution to the following problem:

$$\text{given } \phi \in V^H, \text{ find } Q(\phi) \in V^r \text{ s.t. } \mathscr{B}(\phi + Q(\phi)) - f \in (V^r)^o. \tag{2.5}$$

The correction operator acts on a function $\phi \in V$ and produces a function $Q(\phi) \in V^r$ such that $\phi + Q(\phi)$ now contains information about the solution to the problem posed on V (2.1). To make this precise, define the reconstruction operator $R : V^H \to V$ as $R = Id + Q$, then define the 'ambulant' space

$$V^A = \text{span}\{R(\phi_i) | \{\phi_i\}_{i=1}^{N_H} \text{ is a basis for } V^H\}. \tag{2.6}$$

As we will show shortly, the ambulant space contains the true solution to the model problem (2.1). To see this, consider the Petrov-Galerkin problem where we use the ambulant space as the trial space and the original approximation space V^H as the test space:

$$\text{find } u^A \in V^A \ : \ \mathscr{B}u^A - f \in (V^H)^o. \tag{2.7}$$

Lemma 2.0.1. *Problems* (2.1) *and* (2.7) *are equivalent.*

Proof. Write $u^A = R(u^H)$ for some $u^H \in V^H$ and let $\phi \in V$ be an arbitrary test function. Then $\phi = \phi^H + \phi^r$ for some $\phi^H \in V^H$ and $\phi^r \in V^r$.

We know from (2.7)

$$\mathscr{B}u^A(\phi^H) - f(\phi^H) = 0, \tag{2.8}$$

and

$$\mathscr{B}R(u^H)(\phi^r) - f(\phi^r) = 0, \tag{2.9}$$

from the definition of Q. Summing these two equations yields that $u^A = R(u^H)$ solves

$$\mathscr{B}u^A(\phi) - f(\phi) = 0, \tag{2.10}$$

the original problem. Since Lax-Milgram guarantees a unique solution to both problems we have $u^A = u$. □

Additionally, we can state the standard Galerkin problem on V^A and obtain a similar result:

$$\text{find } u \in V^A \text{ s.t. } \mathscr{B}u - f \in (V^A)^o. \tag{2.11}$$

Lemma 2.0.2. *Problems* (2.1) *and* (2.11) *are equivalent.*

Proof. This Lemma is a direct consequence of Lemma 2.0.1 and the best approximation property of the Galerkin method. Define u^A as the solution to (2.11) and u as the solution to (2.1). Clearly $V^A \subset V$ is a closed subspace of V. Denote by α the coercivity constant associated with the operator $\mathscr{B}$ and C the continuity constant associated with the operator $\mathscr{B}$. Then, by the standard best approximation property of the Galerkin method, we have,

$$\|u - u^A\|_V \leq \frac{C}{\alpha} \inf_{v \in V^A} \|u - v\|_V. \tag{2.12}$$

Since $u \in V^A$ by Lemma 2.0.1, we have

$$\|u - u^A\|_V = 0. \tag{2.13}$$

□

2.1 Ambulant Approximations

Lemmas 2.0.1 and 2.0.2 point out that while (2.7) and (2.11) are formally finite dimensional, the dependence of Q on the dimension of V^r results in infinite dimensional problems. In this section we consider finite dimensional approximations of the operator Q and the convergence of the corresponding methods in the Galerkin and Petrov-Galerkin settings.

To design finite dimensional approximations, we introduce a family of finite dimensional spaces $\{V^a \mid a > 0\}$ such that

$$V \supset V^a \supset V^H, \quad \forall a. \tag{2.14}$$

To assist with the convergence analysis we make a sensible assumption on the family of spaces $\{V^a\}$,

Assumption 2.1.1. *The family $\{V^a\}_a$ is dense in V in the sense that for each $v \in V$ there exists a sequence $\{v_n \in V^{a_n}\}$ with $a_n \to 0$ as $n \to \infty$ such that*

$$\|v - v_n\|_V \to 0 \text{ as } n \to \infty. \tag{2.15}$$

Choosing a particular a, we then we set

$$V^{r,a} = Ker(I^H|_{V^a}). \tag{2.16}$$

Then we define the ambulant approximation space V^{A_a} by the basis functions $\{R^a(\phi_i)\}_{i=1}^{N_H}$ where $R^a = Id + Q^a$ and $Q^a(\phi_i)$ is the solution to the problem,

$$\text{find } Q^a(\phi_i) \in V^{r,a} \text{ s.t. } \mathscr{B}(\phi_i + Q^a(\phi_i)) - f \in (V^{r,a})^o. \tag{2.17}$$

Next we show that under Assumption 2.1.1 the family $\{V^{r,a}\}_a$ is dense in V^r.

Proposition 2.1.1. *Under Assumption 2.1.1, we have additionally that the family* $\{V^{r,a}\}_a$ *is dense in* V^r *in the sense that for each* $v \in V^r$ *there exists a sequence* $\{v_n \in V^{r,a_n}\}$ *with* $a_n \to 0$ *as* $n \to \infty$ *such that*

$$\|v - v_n\|_V \to 0 \text{ as } n \to \infty. \tag{2.18}$$

Proof. Let $v \in V^r \subset V$ and let $\{v_n \in V^{a_n}\}_{n=1}^{\infty}$ with $a_n \to 0$ as $n \to \infty$ be the sequence guaranteed by Assumption 2.1.1 to converge in V to the element $v \in V^r$. We note that each v_n can be written as

$$v_n = v_n^H + v_n^r, \tag{2.19}$$

where $v_n^H = I^H(v_n)$. Similarly we may write $v = v^H + v^r$. Thus,

$$\lim_{n\to\infty} \|v - v_n\|_V = \lim_{n\to\infty} \|v^H - v_n^H + v^r - v_n^r\|_V = 0. \tag{2.20}$$

And so we have

$$\|v^r - v_n^r\|_V \to 0 \text{ as } n \to \infty. \tag{2.21}$$

Since $v \in V^r$, we also have $v^H = 0$ and $v = v^r$, so that the sequence $\{v_n^r = v_n - I^H(v_n) \in V^{r,a_n}\}_{n=1}^{\infty}$ is the sequence we seek. Note that $v \in V^r$ was chosen arbitrarily, and so we have the result. □

In the convergence proofs to follow we need to know that as $a \to 0$, $R^a(\phi) \to R(\phi)$ in V for any function $\phi \in V^H$. We demonstrate this in the next theorem.

Theorem 2.1.1. *Let* $\phi \in V^H$. *Under Assumption 2.1.1,*

$$\|R(\phi) - R^a(\phi)\|_V \to 0 \text{ as } a \to 0. \tag{2.22}$$

Proof. We begin by restructuring the problems (2.5) and (2.17). Let $g = f - \mathscr{B}\phi \in V'$. Then (2.5) and (2.17) can be written as,

$$\text{find } q \in V^r \text{ s.t. } \mathscr{B}q - g \in (V^r)^o, \tag{2.23}$$

and

$$\text{find } q^a \in V^{r,a} \text{ s.t. } \mathscr{B}q^a - g \in (V^{r,a})^o. \tag{2.24}$$

Parts of this proof are similar to the standard best approximation property of the Ritz-Galerkin approximation. In particular, we begin with Galerkin orthogonality, noting that since $V^{r,a} \subset V^r$, subtracting (2.23) from (2.24), we have

$$\mathscr{B}(q^a - q) \in (V^{r,a})^o. \tag{2.25}$$

Then, denoting α the coercivity constant for the operator $\mathscr{B}$ and C the continuity constant, we have, for any $v^a \in V^{r,a}$,

$$\begin{aligned}
\alpha\|q-q^a\|_V^2 &\leq \mathscr{B}(q-q^a)(q-q^a) && (2.26)\\
&= \mathscr{B}(q-q^a)(q) - \mathscr{B}(q-q^a)(q^a) && (2.27)\\
&= \mathscr{B}(q-q^a)(q) && (2.28)\\
&= \mathscr{B}(q-q^a)(q) - \mathscr{B}(q-q^a)(v^a) && (2.29)\\
&= \mathscr{B}(q-q^a)(q-v^a) && (2.30)\\
&\leq C\|q-q^a\|_V\|q-v^a\|_V. && (2.31)
\end{aligned}$$

So,

$$\|q-q^a\|_V \leq \frac{C}{\alpha}\inf_{v^a\in V^a}\|q-v^a\|_V. \tag{2.32}$$

Then by Proposition 2.1.1, we have

$$\|q-q^a\|_V \to 0 \quad \text{as } a\to 0. \tag{2.33}$$

Finally we note that

$$\begin{aligned}
\|R(\phi)-R^a(\phi)\|_V &= \|\phi+Q(\phi)-\phi-Q^a(\phi)\|_V\\
&= \|\phi+q-\phi-q^a\|_V = \|q-q^a\|_V. && (2.34)
\end{aligned}$$

And so,

$$\|R(\phi)-R^a(\phi)\|_V \to 0 \text{ as } a\to 0. \tag{2.35}$$

□

2.1.1 Petrov-Galerkin Formulation

With the finite dimensional approximation operator Q^a at hand we can define the Ambulant Petrov-Galerkin problem,

$$\text{find } u^{pg}\in V^{A_a} \text{ s.t. } \mathscr{B}u^{pg}-f\in (V^H)^o. \tag{2.36}$$

We would like to know that the Ambulant Petrov-Galerkin method converges to the true solution as $a\to 0$. For clarity of notation, define

$$\phi_i^A = R(\phi_i), \qquad \phi_i^{A_a} = R^a(\phi_i), \tag{2.37}$$

so that we have,

$$V^A = \text{span}\{\phi_i^A\}_i^{N_H}, \qquad V^{A_a} = \text{span}\{\phi_i^{A_a}\}_i^{N_H}. \tag{2.38}$$

Then we may write

$$u^A = \sum_{i=1}^{N_H} u_i \phi_i^A, \qquad u^{pg} = \sum_{i=1}^{N_H} u_i^{pg} \phi_i^{A_a}. \tag{2.39}$$

Thanks to Lemma 2.0.1, we need to understand the error

$$\left\| \sum_{i=1}^{N_H} \left[u_i \phi_i^A - u_i^{pg} \phi_i^{A_a} \right] \right\|_V. \tag{2.40}$$

After applying the triangle inequality, we consider the error, for each i,

$$\|u_i \phi_i^A - u_i^{pg} \phi_i^{A_a}\|_V. \tag{2.41}$$

Proposition 2.1.2. *If $\phi_i^{A_a} \to \phi_i^A$ as $a \to 0$ for each i, then $u^{pg} \to u^A$ in V, i.e.*

$$\|u^A - u^{pg}\|_V \to 0 \text{ as } a \to 0. \tag{2.42}$$

Proof. To prove this we write the out the linear systems corresponding to (2.7) and (2.36). Define $\mathbf{B} \in \mathbb{R}^{N_H \times N_H}$, $\mathbf{B}^{pg} \in \mathbb{R}^{N_H \times N_H}$, and $\mathbf{F} \in \mathbb{R}^{N_H}$ by

$$\mathbf{B}_{i,j} = \mathscr{B}\phi_i^A(\phi_j), \tag{2.43}$$

$$\mathbf{B}_{i,j}^{pg} = \mathscr{B}\phi_i^{A_a}(\phi_j), \tag{2.44}$$

$$\mathbf{F}_j = f(\phi_j). \tag{2.45}$$

Let $\mathbf{u} = [u_1, \ldots, u_{N_H}]^T$ and $\mathbf{u}^{pg} = [u_1^{pg}, \ldots, u_{N_H}^{pg}]^T$. Then we have,

$$\mathbf{B}\mathbf{u} = \mathbf{F}, \tag{2.46}$$

and

$$\mathbf{B}^{pg}\mathbf{u}^{pg} = \mathbf{F}. \tag{2.47}$$

Thus,

$$\mathbf{B}\mathbf{u} = \mathbf{B}^{pg}\mathbf{u}^{pg}, \quad \forall a. \tag{2.48}$$

Then we note that $\lim_{a\to 0} \mathbf{B}^{pg}$ is defined by

$$\left(\lim_{a\to 0} \mathbf{B}^{pg} \right)_{i,j} = \lim_{a\to 0} \mathscr{B}\phi_i^{A_a}(\phi_j). \tag{2.49}$$

Since $\mathscr{B} \in \mathscr{L}(V, V')$, i.e. it is continuous, we have, applying Theorem 2.1.1,

$$\lim_{a\to 0} \mathscr{B}\phi_i^{A_a}(\phi_j) = \mathscr{B}\left(\lim_{a\to 0} \phi_i^{A_a} \right)(\phi_j) \tag{2.50}$$

$$= \mathscr{B}\phi_i^A(\phi_j), \tag{2.51}$$

and so,

$$\lim_{a\to 0} \mathbf{B}^{pg} = \mathbf{B}. \tag{2.52}$$

Then

$$\lim_{a\to 0} \mathbf{B}^{pg}\mathbf{u}^{pg} = \mathbf{B}\lim_{a\to 0} \mathbf{u}^{pg} = \mathbf{B}\mathbf{u}. \tag{2.53}$$

Since $\mathbf{B}$ is invertible, we see that

$$\lim_{a\to 0} \mathbf{u}^{pg} = \mathbf{u}. \tag{2.54}$$

The result follows. □

Theorem 2.1.2. *Under Assumption 2.1.1 we have,*

$$\lim_{a\to 0} \|u - u^{pg}\|_V = 0. \tag{2.55}$$

Proof. By Lemma 2.0.1,

$$\|u - u^{pg}\|_V = \|u^A - u^{pg}\|_V \quad \forall a. \tag{2.56}$$

By Theorem 2.1.1, we have $\phi_i^{A_a} \to \phi_i^A$ in V as $a \to 0$ for each i. Then by Proposition 2.1.2 we have the result,

$$\|u - u^{pg}\|_V \to 0 \text{ as } a \to 0. \tag{2.57}$$

□

So, we see that without changing the approximation space V^H, we can converge to the true solution with refinement only in the residual space $V^{r,a}$.

2.1.2 Galerkin Formulation

Next we consider the finite dimensional Ambulant Galerkin problem,

$$\text{find } u^g \in V^{A_a} \text{ s.t. } \mathscr{B}u^g - f \in (V^{A_a})^o. \tag{2.58}$$

The convergence of this formulation will in fact be a direct consequence of the earlier convergence analysis for the Petrov-Galerkin formulation.

Theorem 2.1.3. *Under Assumption 2.1.1 we have,*

$$\lim_{a\to 0} \|u - u^g\|_V = 0. \tag{2.59}$$

Proof. We first define $\hat{u}$ as the solution of Galerkin problem (2.11). By Lemma 2.0.2 we know that we need only consider the limit,

$$\lim_{a\to 0} \|\hat{u} - u^g\|_V. \tag{2.60}$$

We note that Proposition 2.1.2 is easily extended to the standard Galerkin framework. Indeed this requires nothing more than noting that for each $u \in V$, $\mathscr{B}u \in V'$ is continuous, and passing the limit to both terms in $\lim_{a\to 0} \mathscr{B}\phi_i^{A_a}(\phi_j^{A_a})$. We already saw in Theorem 2.1.1 that

$$\|R(\phi_i) - R^a(\phi_i)\|_V = \|\phi_i^A - \phi_i^{A_a}\|_V \to 0 \qquad \text{as } a \to 0, \quad \forall i. \tag{2.61}$$

Combining these two observations we have the result. □

2.2 Matrix Translation

In this section we examine how the finite dimensional Ambulant problems translate the linear system corresponding to an approximation of the model problem (2.1) on V^H. First we precisely define all relevant operators. We refer to the dimension of the space $V^{r,a}$ by N_a, and let $\{\psi_j\}_{j=1}^{N_a}$ be a basis for this space. We then denote by w_{ij} the weights on $Q(\phi_i)$ in the space $V^{r,a}$,

$$\phi_i^A = \phi_i + \sum_{j=1}^{N_a} w_{ij}\psi_j. \tag{2.62}$$

Then we define the following matrices,

$$\mathbf{B}^H \in \mathbb{R}^{N_H\times N_H} \ : \ \mathbf{B}^H_{ij} = \mathscr{B}\phi_i(\phi_j), \tag{2.63}$$
$$\mathbf{B}^{pg} \in \mathbb{R}^{N_H\times N_H} \ : \ \mathbf{B}^{pg}_{ij} = \mathscr{B}\phi_i^{A_a}(\phi_j), \tag{2.64}$$
$$\mathbf{B}^{g} \in \mathbb{R}^{N_H\times N_H} \ : \ \mathbf{B}^{g}_{ij} = \mathscr{B}\phi_i^{A_a}(\phi_j^{A_a}), \tag{2.65}$$
$$\mathbf{B}^{r,a} \in \mathbb{R}^{N_a\times N_a} \ : \ \mathbf{B}^{r,a}_{ij} = \mathscr{B}\psi_i(\psi_j), \tag{2.66}$$
$$\mathbf{B}^{L} \in \mathbb{R}^{N_a\times N_H} \ : \ \mathbf{B}^{L}_{ij} = \mathscr{B}\psi_i(\phi_j), \tag{2.67}$$
$$\mathbf{B}^{R} \in \mathbb{R}^{N_H\times N_a} \ : \ \mathbf{B}^{R}_{ij} = \mathscr{B}\phi_i(\psi_j), \tag{2.68}$$
$$\mathbf{W} \in \mathbb{R}^{N_H\times N_a} \ : \ \mathbf{W}_{ij} = w_{ij}. \tag{2.69}$$

We see that $\mathbf{B}^H$ is the matrix corresponding to the problem on the approximation space V^H with no correction. $\mathbf{B}^{pg}$, as defined previously is the matrix corresponding to the Petrov-Galerkin formulation of the ambulant problem (2.36). $\mathbf{B}^g$ corresponds to the standard Galerkin formulation of the ambulant problem (2.58). $\mathbf{B}^{r,a}$ corresponds to the problem posed on $V^{r,a}$. $\mathbf{B}^L$ corresponds to a problem whose trial space is V^H and test space is $V^{r,a}$, and visa-versa for $\mathbf{B}^R$. Finally $\mathbf{W}$ is a non-square matrix of coefficients for the multiscale basis functions in $V^{r,a}$.

2.2.1 Petrov-Galerkin Formulation

Here we examine how $\mathbf{B}^{pg}$ is related to $\mathbf{B}^H$. We begin by considering position (i, j) of the ambulant matrix $\mathbf{B}^{pg}$,

$$\begin{aligned}\mathscr{B}\phi_i^{A_a}(\phi_j) &= \mathscr{B}\left(\phi_i + \sum_{l=1}^{N_a} w_{il}\psi_l\right)(\phi_j) \\ &= \mathscr{B}\phi_i(\phi_j) + \sum_{l=1}^{N_a} w_{il}\mathscr{B}\psi_l(\phi_j).\end{aligned}$$

So we see that

$$\mathbf{B}^{pg} = \mathbf{B}^H + \mathbf{W}\mathbf{B}^L. \tag{2.70}$$

2.2.2 Galerkin Formulation

For the Galerkin problem the question is how $\mathbf{B}^g$ is related to $\mathbf{B}^H$. We begin by considering position (i, j) of the ambulant matrix $\mathbf{B}^g$,

$$\begin{aligned}\mathscr{B}\phi_i^{A_a}(\phi_j^{A_a}) &= \mathscr{B}\left(\phi_i + \sum_{l=1}^{N_a} w_{il}\psi_l\right)\left(\phi_j + \sum_{k=1}^{N_a} w_{jk}\psi_k\right) \\ &= \mathscr{B}\phi_i(\phi_j) + \sum_{k=1}^{N_a} w_{jk}\mathscr{B}\phi_i(\psi_k) + \sum_{l=1}^{N_a} w_{il}\mathscr{B}\psi_l(\phi_j) + \sum_{l=1}^{N_a}\sum_{k=1}^{N_a} w_{il}w_{jk}\mathscr{B}\psi_l(\psi_k).\end{aligned}$$

Then we have,

$$\mathbf{B}^g = \mathbf{B}^H + \mathbf{B}^R\mathbf{W}^T + \mathbf{W}\mathbf{B}^L + \mathbf{W}\mathbf{B}^{r,a}\mathbf{W}^T. \tag{2.71}$$

2.3 Reduced Order Modeling Connections

The Ambulant Galerkin framework can also be examined in the context of reduced order modeling (ROM). The question in this context is slightly different than how the AGM has been described earlier. Rather than asking how AGM corrects the V^H space, the ROM question is: how does AGM reduce the V^a space.

To see the connection between ROM and AGM, we first need a basis for the space V^a. But, this is trivial since $V^a = V^H \oplus V^{r,a}$ and we have at hand a basis for V^H as well as for $V^{r,a}$. Let $N = N_H + N_a$, then define the basis $\{\theta_i\}_{i=1}^N$ for V^a by,

$$\theta_i = \begin{cases} \phi_i & 1 \le i \le N_H \\ \psi_{i-N_H} & N_H + 1 \le i \le N. \end{cases} \tag{2.72}$$

Then define the matrix,

$$\mathbb{B} \in \mathbb{R}^{N\times N} \; : \; \mathbb{B}_{ij} = \mathscr{B}\theta_i(\theta_j), \tag{2.73}$$

which corresponds to the solution of the problem on V^a. Next we define an expanded matrix of coefficients, $\mathbb{W}$,

$$\mathbb{W} \in \mathbb{R}^{N_H\times N} \; : \; \mathbb{W}_{ij} = \begin{cases} \delta_{ij} & j \le N_H \\ w_{i(j-N_H)} & j > N_H. \end{cases} . \tag{2.74}$$

So, in blocks we have,

$$\mathbb{B} = \begin{pmatrix} \mathbf{B}^H & \mathbf{B}^R \\ \mathbf{B}^L & \mathbf{B}^{r,a} \end{pmatrix} \tag{2.75}$$

$$\mathbb{W} = \begin{pmatrix} \mathbf{I}_{N_H} \\ \mathbf{W} \end{pmatrix}. \tag{2.76}$$

Then, in the standard Galerkin formulation (2.58), we have

$$\begin{aligned} \mathbf{B}^g_{ij} &= \mathscr{B}\phi_i^{A_a}(\phi_j^{A_a}) \\ &= \sum_{l=1}^{N}\sum_{k=1}^{N} \mathbb{W}_{il}\mathbb{W}_{jk}\mathscr{B}\theta_l(\theta_k) \\ &= \sum_{l=1}^{N}\sum_{k=1}^{N} \mathbb{W}_{il}\mathbb{W}_{jk}\mathbb{B}_{lk}. \end{aligned}$$

And so,

$$\mathbf{B}^g = \mathbb{W}\mathbb{B}\mathbb{W}^T. \tag{2.77}$$

While in the Petrov-Galerkin formulation (2.36), we have

$$\begin{aligned} \mathbf{B}^{pg}_{ij} &= \mathscr{B}\phi_i^{A_a}(\phi_j) \\ &= \sum_{l=1}^{N} \mathbb{W}_{il}\mathscr{B}\theta_l(\phi_j). \end{aligned}$$

Defining the matrix

$$\mathbb{I}_0 \in \mathbb{R}^{N\times N_H} \; : \; \mathbb{I}_0 = \begin{pmatrix} \mathbf{I}_{N_H} \\ \mathbf{0} \end{pmatrix}, \tag{2.78}$$

we then have

$$\mathbf{B}^{pg} = \mathbb{W}\mathbb{B}\mathbb{I}_0^T. \tag{2.79}$$

2.4 Source Removal

In this section we analyze the error induced by removing the source term f from the calculation of the ambulant basis functions in the abstract framework. Thus we replace (2.17) with

$$\text{find } Q^a_*(\phi_i) \in V^{r,a} \text{ s.t. } \mathscr{B}(\phi_i + Q^a_*(\phi_i)) \in (V^{r,a})^o. \tag{2.80}$$

There are several reasons one may be interested in removing the source term. First, as we will see, in the multiscale finite element context we are interested in obtaining basis functions that correspond to material heterogeneity, not to larger scale force variations. Removing the source term encourages the computed basis functions to respond solely to the material parameters within $\mathscr{B}$. Additionally, we have the following result stating that with no source the reconstruction operator is an orthogonality preserving map.

Proposition 2.4.1. *Applying the Riesz Representation Theorem, write $\mathscr{B}u(v) = (\mathscr{B}u, v)_V$, so that in* (2.80) *$\mathscr{B} : V^{r,a} \to V^{r,a}$. Assume $\mathscr{B}$ is a self-adjoint operator. Define $R^a_* = Id + Q^a_*$ where Q^a_* is given by* (2.80)*. Then R^a_* preserves orthogonality. In particular, if $\{\phi_i\}_{i=1}^{N_H}$ is an orthogonal basis for V^H, then $\{R^a_*(\phi_i)\}_{i=1}^{N_H}$ is an orthogonal basis for V^{A_a}.*

Proof. Let $u, v \in V^H$ such that $(u,v)_V = 0$. Then we compute,

$$\begin{aligned}(R^a_*(u), R^a_*(v))_V &= (u + Q^a_*(u), v + Q^a_*(v))_V \\ &= (u,v)_V + (u, Q^a_*(v))_V + (Q^a_*(u), v)_V + (Q^a_*(u), Q^a_*(v))_V.\end{aligned}$$

By assumption we have $(u,v)_V = 0$, and so the first term disappears. Next we note that $u, v \in V^H$ and $Q^a_*(u), Q^a_*(v) \in V^r$. Since $V^r = Ker(I^H)$, $V^H = Im(I^H)$, and I^H is an orthogonal projection, the second two terms vanish, and we are left with

$$(R^a_*(u), R^a_*(v))_V = (Q^a_*(u), Q^a_*(v))_V.$$

In the following $\mathscr{B}^*$ denotes the adjoint of $\mathscr{B}$. Continuing, we have,

$$\begin{aligned}(Q^a_*(u), Q^a_*(v))_V &= (\mathscr{B}\mathscr{B}^{-1} Q^a_*(u), Q^a_*(v))_V \\ &= (\mathscr{B}^{-1} Q^a_*(u), \mathscr{B}^* Q^a_*(v))_V \\ &= (\mathscr{B}^{-1} Q^a_*(u), \mathscr{B} Q^a_*(v))_V.\end{aligned}$$

Then (2.80) tells us,

$$(w, \mathscr{B} Q^a_*(v)) = -(w, \mathscr{B} v)$$

for all $w \in V^{r,a}$. So,

$$\begin{aligned}(\mathscr{B}^{-1} Q^a_*(u), \mathscr{B} Q^a_*(v))_V &= -(\mathscr{B}^{-1} Q^a_*(u), \mathscr{B} v)_V \\ &= -(\mathscr{B}^* \mathscr{B}^{-1} Q^a_*(u), v)_V \\ &= -(Q^a_*(u), v)_V \\ &= 0.\end{aligned}$$

Thus we have

$$(R^a_*(u), R^a_*(v))_V = 0 \text{ for any } u, v \in V^H \text{ with } (u,v)_V = 0.$$

□

Now consider the difference,

$$\begin{aligned}\alpha\|R^a_*(\phi_i) - R^a(\phi_i)\|^2_V &\leq (\mathscr{B}(R^a_*(\phi_i) - R^a(\phi_i)), R^a_*(\phi_i) - R^a(\phi_i))_V \\ &= (\mathscr{B}R^a_*(\phi_i), R^a_*(\phi_i))_V - (\mathscr{B}R^a_*(\phi_i), R^a(\phi_i))_V \\ &\quad - (\mathscr{B}R^a(\phi_i), R^a_*(\phi_i))_V + (\mathscr{B}R^a(\phi_i), R^a(\phi_i))_V. \end{aligned} \tag{2.81}$$

For the first term in the right hand side of (2.81) we have,

$$\begin{aligned}(\mathscr{B}R^a_*(\phi_i), R^a_*(\phi_i))_V &= (\mathscr{B}\phi_i, \phi_i)_V + (\mathscr{B}Q^a_*(\phi_i), \phi_i)_V \\ &\quad + (\mathscr{B}\phi_i, Q^a_*(\phi_i))_V + (\mathscr{B}Q^a_*(\phi_i), Q^a_*(\phi_i))_V. \end{aligned} \tag{2.82}$$

In the second term, we have,

$$\begin{aligned}(\mathscr{B}R^a_*(\phi_i), R^a(\phi_i))_V &= (\mathscr{B}\phi_i, \phi_i)_V + (\mathscr{B}Q^a_*(\phi_i), \phi_i)_V \\ &\quad + (\mathscr{B}\phi_i, Q^a(\phi_i))_V + (\mathscr{B}Q^a_*(\phi_i), Q^a(\phi_i))_V. \end{aligned} \tag{2.83}$$

For the third term, we have,

$$\begin{aligned}(\mathscr{B}R^a(\phi_i), R^a_*(\phi_i))_V &= (\mathscr{B}\phi_i, \phi_i)_V + (\mathscr{B}Q^a(\phi_i), \phi_i)_V \\ &\quad + (\mathscr{B}\phi_i, Q^a_*(\phi_i))_V + (\mathscr{B}Q^a(\phi_i), Q^a_*(\phi_i))_V. \end{aligned} \tag{2.84}$$

And finally for the fourth term, we have,

$$\begin{aligned}(\mathscr{B}R^a(\phi_i), R^a(\phi_i))_V &= (\mathscr{B}\phi_i, \phi_i)_V + (\mathscr{B}Q^a(\phi_i), \phi_i)_V \\ &\quad + (\mathscr{B}\phi_i, Q^a(\phi_i))_V + (\mathscr{B}Q^a(\phi_i), Q^a(\phi_i))_V. \end{aligned} \tag{2.85}$$

Combining these, with cancellations, we have,

$$\alpha\|R^a_*(\phi_i) - R^a(\phi_i)\|^2_V \leq (\mathscr{B}Q^a_*(\phi_i), Q^a_*(\phi_i) - Q^a(\phi_i))_V + (\mathscr{B}Q^a(\phi_i), Q^a(\phi_i) - Q^a_*(\phi_i))_V. \tag{2.86}$$

Then applying (2.17) and (2.80) we have,

$$\begin{aligned}\alpha\|R^a_*(\phi_i) - R^a(\phi_i)\|^2_V &\leq -(\mathscr{B}\phi_i, Q^a_*(\phi_i))_V + (\mathscr{B}\phi_i, Q^a(\phi_i))_V \\ &\quad - (\mathscr{B}\phi_i, Q^a(\phi_i))_V + (f, Q^a(\phi_i))_V \\ &\quad + (\mathscr{B}\phi_i, Q^a_*(\phi_i))_V - (f, Q^a_*(\phi_i))_V. \end{aligned}$$

And so,

$$\alpha\|R^a_*(\phi_i) - R^a(\phi_i)\|^2_V \leq (f, Q^a(\phi_i) - Q^a_*(\phi_i))_V. \tag{2.87}$$

In the finite element context, where ϕ_i has support determined by the mesh size in V^H, we see that the error induced by dropping the source term will be on the order of the mesh size in V^H.

Chapter 3

Peridynamic Model of Continuum Mechanics

The peridynamic theory of continuum mechanics is a nonlocal theory that remains valid in the presence of discontinuities. The theory has several advantages over the traditional theory, including natural modeling of material failure, validity across a wide range of scales, and the ability to model nonlocal effects.

The original peridynamic theory (bond-based peridynamics) was introduced by S.A. Silling in 2000 [35]. In 2007 [32] Silling et al. introduced the state-based peridynamic model, which significantly enhanced the types of materials the theory is able to model. Significant work has been done on comparing the peridynamic model to discrete models and classical continuum theory. In 2008 [39] Silling and Lehoucq established, under suitable assumptions, the convergence of the peridynamic model to classical elasticity theory in the limit of vanishing nonlocality. Lehoucq and Silling, and Seleson [22, 29] examined the relationship between molecular dynamics and the peridynamic theory, and showed that molecular dynamics is a special case of the peridynamic model when generalized functions are used in the constitutive model. In 2015 Rahman and Foster [25] examined the relationship between statistical mechanics and the peridynamic theory.

Let $D \subset \mathbb{R}^d$, $d \in \{1,2,3\}$, denote a material body. The principal assumption in the peridynamic theory is that any body-point x in the reference configuration is acted upon by forces due to interactions with all the body-points q within some neighborhood of finite radius δ. The radius δ is referred to as the *horizon*, and the set of points within this neighborhood is referred to as the *family* of x, typically denoted $\mathscr{H}_x = \{q \in D \mid |q-x| < \delta\}$. In the peridynamic theory, a concise form of the equation of motion is stated as

$$\rho(x)u_{tt}(x,t) = \int_{\mathscr{H}_x} f(q,x,t)\, dq + b(x,t), \quad x \in D,\ t > 0, \tag{3.1}$$

where $\rho(x)$ is the density of the body in a reference configuration, $u(x,t)$ is the displacement field, and b is a prescribed body force density. The first term on the right hand side is the internal force density, and it is here that we see, mathematically, the expression of nonlocality. The internal force density at a point x depends on all points in the family of x. Further, for a given body-point $x \in D$ it is assumed that beyond the horizon, q exerts no force on x. So,

$$|q-x| > \delta \Rightarrow f(q,x,t) = 0. \tag{3.2}$$

The function f contains information about the deformation and the material model, both from the point x and the point q.

In this work we restrict ourselves to a linear peridynamic body, for which (3.1) has the form,

$$\rho(x)u_{tt}(x,t) = \int_D C(x,q)(u(q,t)-u(x,t))\,dq + b(x,t), \tag{3.3}$$

where $C(\cdot,\cdot) : D \times D \to \mathbb{R}^{d\times d}$ is a tensor-valued micro-modulus function which describes the material. We note that the linear peridynamic model assumes small displacements, but does not prohibit fracture. We require that the micromodulus function $C(x,q)$ is symmetric in its arguments so that the integrand is anti-symmetric in accordance with Newton's third law, i.e. the force exerted on q by x is equal and opposite to the force exerted on x by q.

Additionally, nonlocal diffusion and the static peridynamic problems have similar formulations,

$$u_t(x,t) = \int_D C(x,q)(u(q,t)-u(x,t))\,dq + b(x,t), \tag{3.4}$$

$$\int_D C(x,q)(u(q)-u(x))\,dq + b(x,t) = 0. \tag{3.5}$$

For nonlocal diffusion, (3.4), u is scalar valued.

3.1 Weak Formulation of Peridynamics

The weak formulation of the linear peridynamic model is established in the standard way by multiplying by a test function $v \in V$, where V is a Hilbert space yet to be determined, and integrating.

$$\int_D \rho u_{tt} v\,dx - \int_D v \int_D C(x,q)(u(q)-u(x))\,dq\,dx = \int_D bv\,dx. \tag{3.6}$$

Thus we define the bilinear forms,

$$(\cdot,\cdot)_\rho : V\times V \to \mathbb{R} \;:\; (u,v)_\rho = \int_D \rho uv\,dx, \tag{3.7}$$

$$(\cdot,\cdot) : V\times V \to \mathbb{R} \;:\; (u,v) = \int_D uv\,dx, \tag{3.8}$$

$$B_1(\cdot,\cdot) : V\times V \to \mathbb{R} \;:\; B_1(u,v) = -\int_D v \int_D C(x,q)(u(q)-u(x))\,dq\,dx. \tag{3.9}$$

It will be convenient to rewrite B_1 in an equivalent form. Define,

$$B(u,v) = \frac{1}{2}\int_D\int_D C(x,q)(u(q)-u(x))(v(q)-v(x))\,dq\,dx. \tag{3.10}$$

Proposition 3.1.1. *Assume C is $L^2(D)\times L^2(D)$ integrable. Then $B(u,v)=B_1(u,v)$ for all $u,v: D\to\mathbb{R}^d$. In particular, the weak operator corresponding to internal force density for the linear peridynamic model is self-adjoint.*

Proof. Applying Fubini's Theorem to exchange the order of integration in the third step, we have,

$$\begin{aligned}
B(u,v) &= \frac{1}{2}\int_{D\times D} C(x,q)(u(q)-u(x))(v(q)-v(x))\,dq\,dx \\
&= \frac{1}{2}\int_D\int_D C(x,q)(u(q)v(q)-u(q)v(x))\,dq\,dx \\
&\quad + \frac{1}{2}\int_D\int_D C(x,q)(u(x)v(x)-u(x)v(q))\,dq\,dx \\
&= \frac{1}{2}\int_D\int_D C(x,q)(u(x)v(x)-u(q)v(x))\,dq\,dx \\
&\quad + \frac{1}{2}\int_D\int_D C(x,q)(u(x)v(x)-u(q)v(x))\,dq\,dx \\
&= -\int_D\int_D C(x,q)(u(q)-u(x))v(x)\,dq\,dx \\
&= -\int_D v(x)\int_D C(x,q)(u(q)-u(x))\,dq\,dx \\
&= B_1(u,v).
\end{aligned}$$

□

As has been well-established, standard boundary conditions are insufficient for the nonlocal peridynamic model [12, 17]. Instead, we require a volume constraint. To introduce the volume constraint, we define $D_{\mathscr{I}}$, the interaction domain, as

$$D_{\mathscr{I}} = \{x\notin D \,:\, \operatorname{dist}(x,\partial D)\le\delta\}. \tag{3.11}$$

We then define

$$D' = D\cup D_{\mathscr{I}}. \tag{3.12}$$

An illustration of this geometry in $\mathbb{R}^2$ is given in Figure 3.1.

We must make some assumptions on the micromodulus function C to ensure B behaves appropriately when inducing a (semi) norm.

Assumption 3.1.1. *We assume the following:*

1. *C is $L^2(D')\times L^2(D')$ integrable.*
2. *C is non-negative on $D'\times D'$.*
3. *There exist constants $a_0,c_0>0$ such that for each $x\in D'$, there exists $\mathscr{A}_x\subseteq\mathscr{H}_x$ with $|\mathscr{A}_x|\ge a_0$, and $C(x,q)\ge c_0$ for each $q\in\mathscr{A}_x$, and $\{\mathscr{A}_x\}_{x\in D'}$ is a covering of D'.*

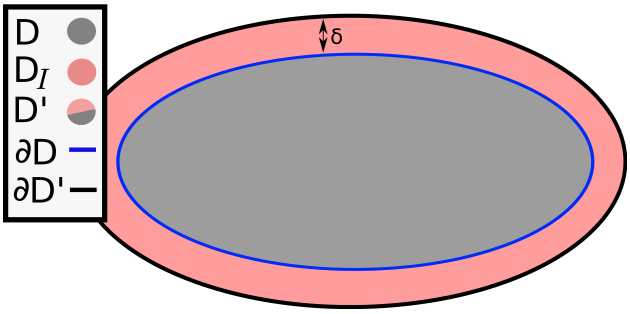

Figure 3.1. Illustration of interaction domain in $\mathbb{R}^2$.

We then define the energy space associated with the linear peridynamic problem,

$$\mathscr{E} = \{w : D' \to \mathbb{R}^d \ : \ B(w,w) < \infty\}. \tag{3.13}$$

Under assumption 3.1.1 we see that B is a semi-inner product on $\mathscr{E}$ and

$$|w|_{\mathscr{E}} = (B(w,w))^{\frac{1}{2}} \tag{3.14}$$

is a semi-norm. We note that B does not induce a full inner product and norm on $\mathscr{E}$. For any function $w : D' \to \mathbb{R}^d$ that is constant almost everywhere we will have $B(w,w) = |w|^2_{\mathscr{E}} = 0$. This is analogous to the problem that arises with the bilinear form corresponding to the linear Poisson equation posed on H^1. The space $\mathscr{E}$ needs to be clamped down in the interaction domain in order to ensure positive-definiteness. So we define,

$$V = \{w \in \mathscr{E} \ : \ w|_{D_{\mathscr{I}}} = 0\}, \tag{3.15}$$

with the inner product and norm,

$$(u,v)_V = B(u,v), \tag{3.16}$$

$$\|u\|^2_V = B(u,u). \tag{3.17}$$

Finally, we define,

$$W = H^2(0,T;V) := \left\{ v : [0,T] \to V \ \middle| \ \left(\int_0^T \|\partial_t^i v(t)\|^2_V \, dt \right)^{\frac{1}{2}} < \infty, \ \ i = 0,1,2 \right\}. \tag{3.18}$$

Then we have the weak form of the homogeneous Dirichlet linear peridynamic problem,

$$\text{find } u \in W \ : \ (u_{tt}(t),v)_\rho + B(u(t),v) = (b(t),v), \quad \forall v \in V \text{ and a.e. } t \in [0,T]. \tag{3.19}$$

And for the static case,

$$\text{find } u \in V \ : \ B(u,v) = (b,v), \quad \forall v \in V. \tag{3.20}$$

Chapter 4

Peridynamic Multiscale Finite Element Methods

In this section we describe how the AGM framework connects directly to a nonlocal multiscale finite element method for the static peridynamic problem (3.20). We then consider a method that solves a fine-scale peridynamic model to build element-support basis functions for a coarse scale local partial differential equation model, called the Mixed Locality Multiscale Finite Element Method (ML-MSFEM).

4.1 Nonlocal Multiscale Finite Element Method

Let $\mathscr{T}^H = \{T_i\}_{i=1}^N$ be a regular triangulation of the domain D' into intervals ($d = 1$), triangles ($d = 2$), or tetrahedrons ($d = 3$). Here H is the mesh size, and we consider a discontinuous piecewise linear finite element space. We note that a discontinuous Galerkin approximation to the peridynamic problem is conforming [10]. Denote by M the number of basis functions on each element. Let $\{\phi_{i,j}\}$, $i \in \{1,\dots,N\}$ and $j \in \{1,\dots,M\}$ be the basis for the finite element problem, so that $V^H = \text{span}\{\phi_{i,j}\}_{ij}$.

For the space V^a we take the simplest case of a regular mesh refinement of the mesh $\mathscr{T}^H$. Denoting this new mesh by $\mathscr{T}^a$, we have $\mathscr{T}^a = \{Y_{i,k}\}_{ik}$. Throughout, we will use i to refer to a coarse element in $\mathscr{T}^H$, j to index coarse basis functions $\phi_{i,j}$ on each coarse element, and $k \in \{1,\dots,N_i\}$ to index fine elements in the mesh refinement within coarse element i. In this context, a refers to the mesh size of the refined mesh $\mathscr{T}^a$. Finally, on each coarse element T_i, and each fine element $Y_{i,k}$ within T_i, we again define a discontinuous piecewise linear approximation through basis functions $\{\psi_{i,k,l}\}_{ikl}$. Here $l \in \{1,\dots,M\}$ indexes basis functions in the finite element space V^a defined on element $Y_{i,k}$. Figure 4.1 illustrates this setup in 1D. In this setup we have $N_H = M * N$ and $N_a = M\sum_{i=1}^N N_i$.

Then for each pair (i,j) the ambulant basis function $R_*^a(\phi_{i,j}) = \phi_{i,j} + Q_*^a(\phi_{i,j})$ is computed by,

$$B(Q_*^a(\phi_{i,j}), \psi_{i,k,l}) = -B(\phi_{i,j}, \psi_{i^*,k,l}) \quad i^* = 1,\dots,N,\ k = 1,\dots,N_i,\ l = 1,\dots,M. \tag{4.1}$$

Notice that in (4.1) the computations are performed on the entire domain D', and we expect that $R_*^a(\phi_{i,j})$ will have support outside of T_i.

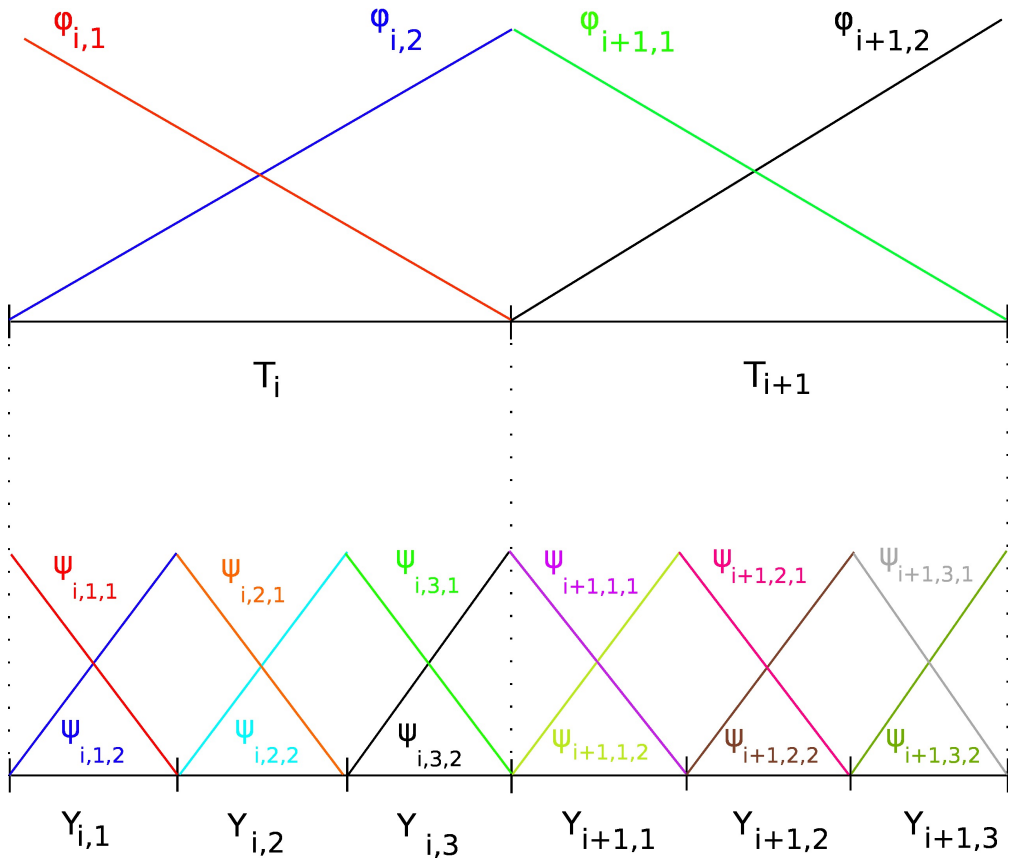

Figure 4.1. Illustration of element and basis indexing in 1D.

To obtain a method that computes $R^a_*(\phi_{i,j})$ locally, we replace (4.1) with

$$B(Q^a_*(\phi_{i,j}), \psi_{i,k,l}) = -B(\phi_{i,j}, \psi_{i,k,l}) \quad k = 1, \ldots, N_i,\ l = 1, \ldots, M. \tag{4.2}$$

We note that the domain T_i for each computation is padded and homogeneous Dirichlet volume constraints are enforced in the padded domain. Then,

$$R^a_*(\phi_{i,j}) = \begin{cases} \phi_{i,j} + Q^a_*(\phi_{i,j}) & x \in T_i \\ 0 & x \notin T_i \end{cases}. \tag{4.3}$$

This method defines a nonlocal multiscale finite element method.

4.2 Mixed Locality Finite Element Method

Due to the relatively high cost of solving the weak peridynamic model compared to finite element methods for local models, as well as the decades of work that has gone into the development of FEM codes for local mechanics models, a natural question to ask is, can we use the multiscale

finite element method to communicate across scales from nonlocal models (fine scale) to (coarse scale) local models of continuum mechanics? We call this method the Mixed Locality Multiscale Finite Element Method (ML-MSFEM), and describe it in this section for a linear elastic material.

The local model corresponding to the linear static peridynamic problem (3.20) is the linear Poisson equation,

$$-\nabla \cdot (\alpha \nabla u) = b, \quad x \in D, \tag{4.4}$$

$$u = 0, \quad x \in \partial D. \tag{4.5}$$

The micromodulus function $C(x,q)$ and the coefficient function $\alpha(x)$ are related by

$$C(x,q) = \frac{\alpha(x) + \alpha(q)}{2}. \tag{4.6}$$

For details regarding the assumptions and scaling necessary to obtain this local model as the 0 horizon limit of the linear peridynamic model, the reader is referred to [39]. In fact, we will ultimately be interested in coupling local and nonlocal models for which this convergence does not hold due to, e.g. fracture.

The method of obtaining the weak form of the problem (4.4)-(4.5) can be found in texts covering Hilbert space methods or the finite element method [7, 31]. The weak form is stated as,

$$\text{find } u \in H_0^1(D) \text{ s.t. } B^{loc}(u,v) = (b,v), \quad \forall v \in H_0^1(D). \tag{4.7}$$

Here

$$H_0^1 = \{v \in L^2(D) \ : \ \partial_i u \in L^2(D),\ i \in \{x,y,z\},\ \gamma u = 0\}, \tag{4.8}$$

where ∂_i refers to the distributional derivative in the i direction and γ is the trace operator. Additionally,

$$H^{-1} = (H_0^1)', \tag{4.9}$$

and

$$B^{loc} : H_0^1(D) \times H_0^1(D) \to \mathbb{R}; \quad B^{loc}(u,v) = \int_D \alpha \nabla u \cdot \nabla v \, dx. \tag{4.10}$$

Then the ML-MSFEM method is composed of two steps. First, for each pair (i,j) the multiscale basis function $R_*^a(\phi_{i,j})$ is computed as in the Nl-MSFEM, by (4.2).

The second step requires a choice. The basis functions $\{R_*^a(\phi_{i,j})\}$ are basis functions for a discontinuous Galerkin (DG) [27] space, which is non-conforming for the local PDE model (4.4)-(4.5). One could then solve (4.7) with a DG method. Alternatively, we can paste the DG basis functions together across edges to create a basis for a continuous Galerkin space. In this paper we do the latter. Analysis of these options and the method in general will be the subject of later work.

This page intentionally left blank.

Chapter 5

Numerical Experiments

In this section we present numerical results for both the nonlocal and mixed-locality multiscale finite element methods.

5.1 Nonlocal Multiscale Finite Elements

In Figures 5.1 and 5.2 we compare results from the standard multiscale finite element method for the linear Poisson equation in 1D,

$$-(\alpha(x)u_x)_x = b, \quad x \in (0,1), \tag{5.1}$$
$$u(0) = u(1) = 0, \tag{5.2}$$

and the nonlocal multiscale finite element method for the corresponding peridynamic problem with horizon $\delta = 0.01$. We set

$$\alpha(x) = (4 + 3\sin(100x))^{-1} \tag{5.3}$$

in the local problem, and

$$C(x,q) = \frac{\alpha(x) + \alpha(q)}{2} \tag{5.4}$$

in the nonlocal problem. For both problems the force density is set to

$$b = 1. \tag{5.5}$$

In Figure 5.1 for the local (a) and nonlocal (b) problem we compare the solutions obtained by: (i) standard FEM with 1000 elements, (ii) standard FEM with 6 elements, and (iii) multiscale FEM with 6 coarse elements and 30 fine elements per coarse element. As expected we see good agreement between the solution on the 6 element multiscale space and the 1000 element standard FEM space in both cases, while the standard FEM solution with 6 elements is very poor.

The three solutions displayed in Figure 5.1 also provide a clear basis for reviewing the advantage of the multiscale finite element method in the context of large-scale next generation computing

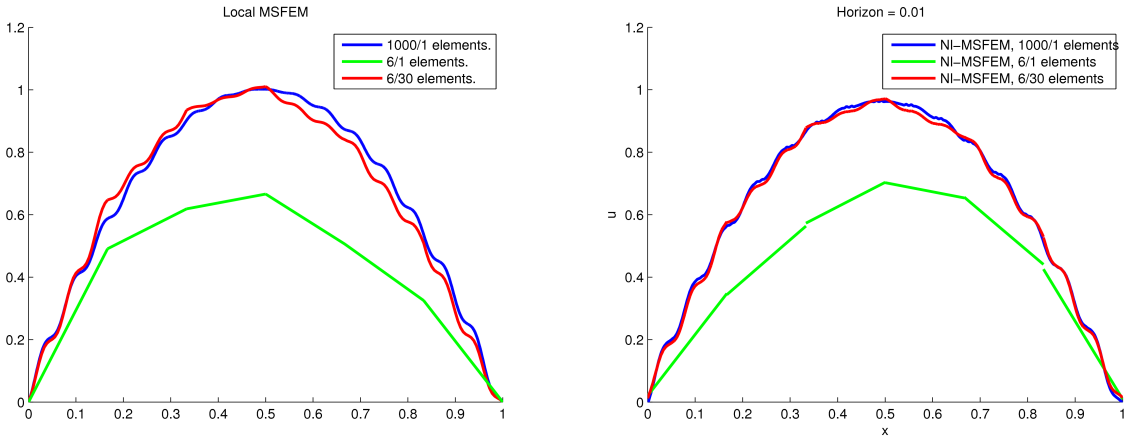

(a) Local multiscale finite element examples.

(b) Nonlocal multiscale finite element examples.

Figure 5.1. Comparison of local and nonlocal multiscale finite element solutions.

platforms. Table 5.1 lists the degrees of freedom in the global solve for each solution as well as the mesh size H. This shows that the MSFEM framework provides an accurate solution with an extremely small global system to solve and a very large mesh size. This is done by shifting the computational burden to the decoupled fine scale problems which produce basis functions. These subscale problems can be computed concurrently, with no communication required between nodes, a clear advantage given the current trends in large scale computing. For the stationary problem the advantages here are clear: a smaller global problem to solve reduces solution time and memory requirements. For dynamic problems there is an additional advantage; for any time stepping scheme that is not fully implicit stability requirements put limitations on the size of the time step taken that are a function of the mesh size. For dynamic problems the MSFEM framework allows larger time steps for explicit and semi-implicit schemes by obtaining accuracy in space through the fine scale solutions while the time step is determined by the global mesh size.

Method	1000/1	6/1	6/30
Global Degrees of Freedom	2000	12	12
Mesh size H	0.001	0.166	0.166.

Table 5.1. Degrees of freedom and mesh size for solutions in Figure 5.1.

In Figure 5.2 we compare the multiscale basis functions computed with the local MSFEM to those computed for the nonlocal problem with increasing horizon, δ. As we expect, when the horizon is below the fine scale mesh size, we see perfect agreement with the local problem, whereas as the horizon is increased past the fine scale mesh size we see disagreement.

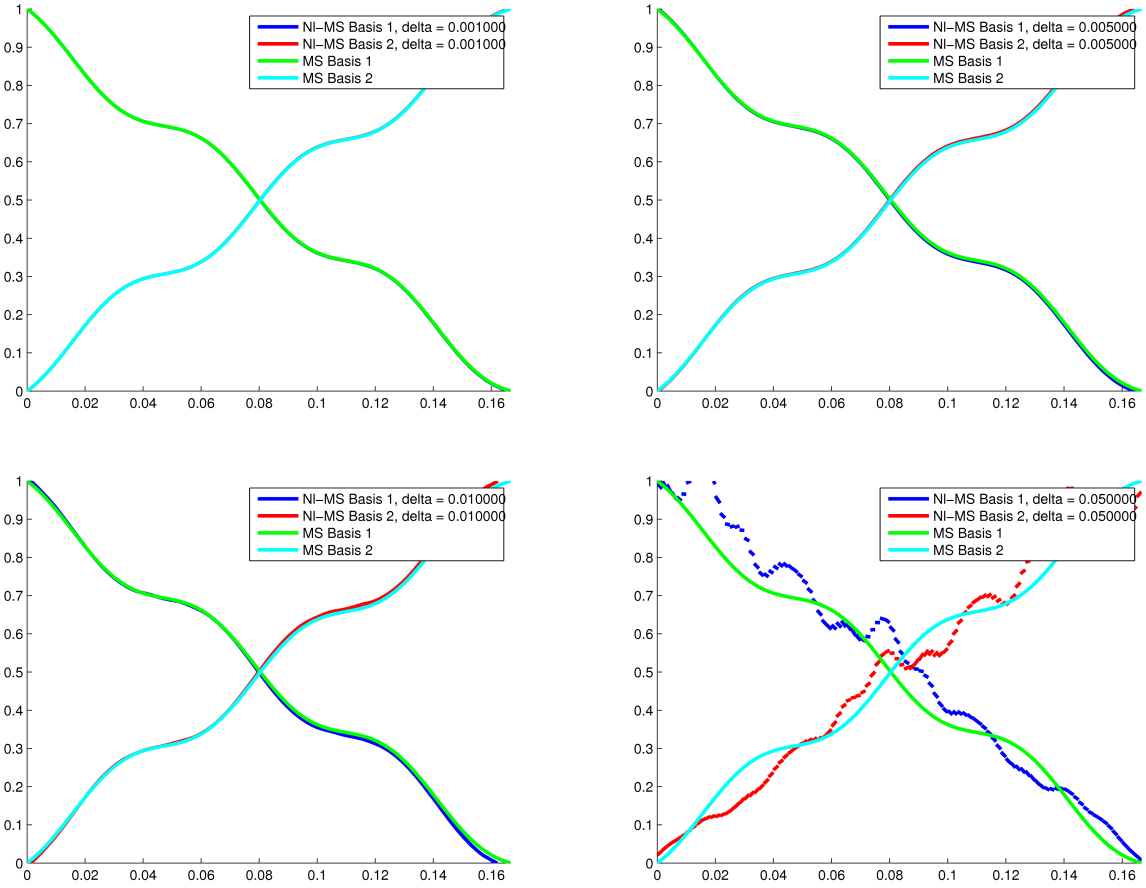

Figure 5.2. Comparison of local and nonlocal MSFEM basis functions for various horizons.

Next we perform convergence tests for the nonlocal multiscale finite element method. In these tests we used the following,

$$u^{exact}(x) = -2x^2 + \frac{x\sin(30\pi x)}{50} + \frac{\cos(30\pi x)}{1500\pi} + 2, \tag{5.6}$$

$$\alpha(x) = \frac{2}{4 - \frac{3}{5}\pi\cos(30\pi x)}. \tag{5.7}$$

In Figure 5.3 we show the convergence as the mesh size H is refined for various fixed numbers of fine scale elements used to produced each multiscale basis function on each coarse element. We see that the standard finite element method corresponding to 1 fine scale element per coarse element fails to achieve the expected convergence rates due to the microscale heterogeneity of the true solution. In contrast, in the Nl-MSFEM tests, for each number of fine scale elements used to compute multiscale basis functions on the coarse mesh we see order 2 convergence. Additionally, we see a drop in the error as the number of fine elements used to compute the multiscale basis functions is increased.

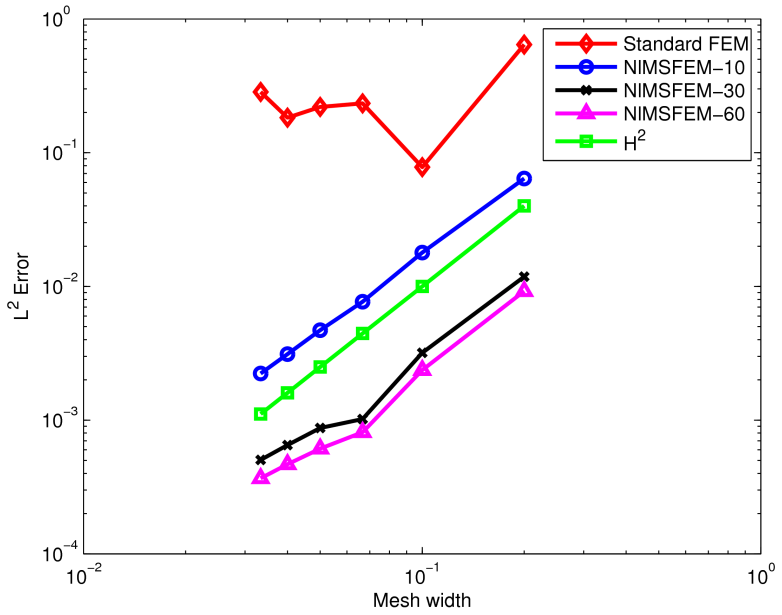

Figure 5.3. *H*-convergence for fixed numbers of fine scale elements used in computing multiscale basis functions on each coarse element. NlMSFEM-M refers to M fine scale elements for each Nl-MSFEM basis function.

5.2 Mixed Locality Multiscale Finite Elements

In this section we present preliminary results from the mixed-locality multiscale finite element method. In Figures 5.4-5.5 we compare results from simulating a problem of periodic microscale heterogeneity with a horizon, $\delta = 0.1$, large enough to create a meaningful difference between the local and nonlocal solutions. It appears, qualitatively, that the ML-MSFEM method reproduces the behavior of the nonlocal solution, despite the coarse global solve being performed with the local model. This is a promising first look at the ML-MSFEM, but needs significant further investigation.

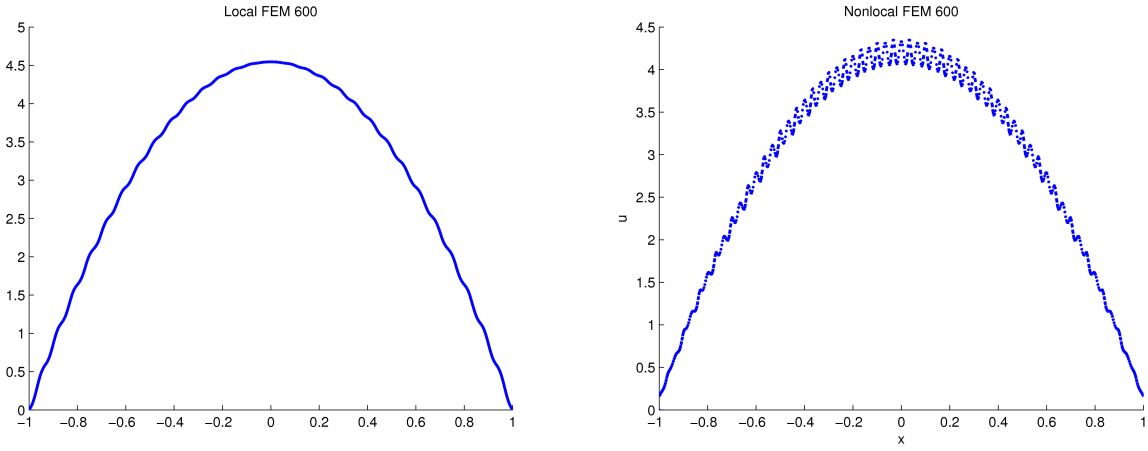

Figure 5.4. Local (left) and Non-local (right) problem solutions with standard FEM with 600 elements.

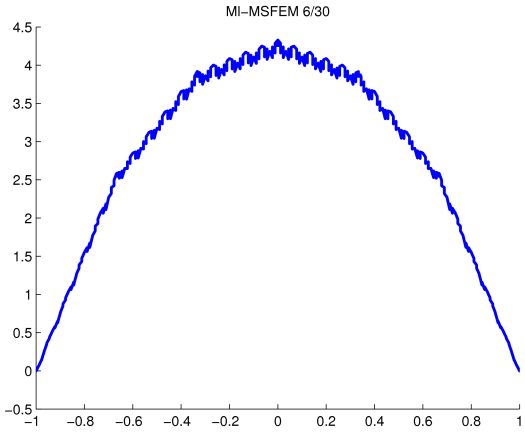

Figure 5.5. Solution with mixed-locality multiscale finite elements with 20 coarse elements and 30 fine elements per coarse element used in basis construction.

This page intentionally left blank.

Chapter 6

Conclusions

In this report we presented preliminary results on a multiscale finite element method for the nonlocal peridynamic theory of continuum mechanics. We presented a novel Galerkin framework intended for a unified analysis of multiscale finite element methods, and demonstrated good performance of the nonlocal and mixed-locality multiscale finite element methods on simple 1D problems that standard finite element methods struggle to solve due to microscale heterogeneity.

The initial results in this report are promising, but much more remains to be done. The analysis of the transition from the Ambulant Galerkin framework to the multiscale finite element framework is encouraging but incomplete. In particular, an error depending on the coarse mesh size H should be discovered in the truncation of the simulation domain for the multiscale basis functions. Also, while the numerical simulations showed that the Nl-MSFEM has H^2 convergence for piece-wise linear microscale basis functions, the analysis in this work demonstrated convergence without an explicit convergence rate. In future work both of these issues will be addressed.

Additionally, analysis of the mixed-locality multiscale finite element method remains to be seen. We anticipate that the asymptotic compatibility framework of Tian and Du [42], combined with the horizon limit convergence results for the peridynamic model [39] will pave the way for extending the AGM framework to allow analysis of the mixed locality multiscale finite element method.

The numerical results in this work were promising, but were restricted to linear problems in 1D. In future work numerical experiments for 2D and 3D problems as well as time dependent and nonlinear problems will be performed. Furthermore, we will implement this method in Sandia's multiphysics finite element code, *Albany/LCM* [28], in combination with the peridynamics code *Peridigm* [23]. We anticipate that the methods described here will be particular useful for time-dependent nonlinear materials for which fully implicit time stepping schemes are not an option, as we expect the stability condition to be dependent on the coarse mesh size H.

Ultimately the goal is to communicate, in a mathematically consistent way, from the quantum scale to design-scale models. In this work we presented preliminary results on an important component of that goal: communicating from the lower limits of the scales of the peridynamic theory of continuum mechanics to nonlocal or local models at the design scale.

This page intentionally left blank.

References

[1] Burak Aksoylu and Michael L Parks. Variational theory and domain decomposition for nonlocal problems. *Applied Mathematics and Computation*, 217(14):6498–6515, 2011.

[2] Bacim Alali and Robert Lipton. Multiscale dynamics of heterogeneous media in the peridynamic formulation. *Journal of Elasticity*, 106(1):71–103, 2012.

[3] E Askari, F Bobaru, RB Lehoucq, ML Parks, SA Silling, and O Weckner. Peridynamics for multiscale materials modeling. In *Journal of Physics: Conference Series*, volume 125. IOP Publishing, 2008.

[4] Albert P. Bartók. *The Gaussian Approximation Potential: An Interatomic Potential Derived from First Principles Quantum Mechanics*. Springer Science & Business Media, 2010.

[5] Albert P Bartók, Mike C Payne, Risi Kondor, and Gábor Csányi. Gaussian approximation potentials: The accuracy of quantum mechanics, without the electrons. *Physical Review Letters*, 104(13):136403, 2010.

[6] José C Bellido and Carlos Mora-Corral. Existence for nonlocal variational problems in peridynamics. *SIAM Journal on Mathematical Analysis*, 46(1):890–916, 2014.

[7] Dietrich Braess. *Finite elements: Theory, fast solvers, and applications in solid mechanics*. Cambridge University Press, 2007.

[8] Haim Brezis. *Functional analysis, Sobolev spaces and partial differential equations*. Springer Science & Business Media, 2010.

[9] CS Chang, H Askes, and LJ Sluys. Higher-order strain/higher-order stress gradient models derived from a discrete microstructure, with application to fracture. *Engineering Fracture Mechanics*, 69(17):1907–1924, 2002.

[10] Xi Chen and Max Gunzburger. Continuous and discontinuous finite element methods for a peridynamics model of mechanics. *Computer Methods in Applied Mechanics and Engineering*, 200(9):1237–1250, 2011.

[11] Qiang Du, Max Gunzburger, Richard B Lehoucq, and Kun Zhou. Analysis and approximation of nonlocal diffusion problems with volume constraints. *SIAM Review*, 54(4):667–696, 2012.

[12] Qiang Du, Max Gunzburger, Richard B Lehoucq, and Kun Zhou. A nonlocal vector calculus, nonlocal volume-constrained problems, and nonlocal balance laws. *Mathematical Models and Methods in Applied Sciences*, 23(03):493–540, 2013.

[13] Qiang Du, Lili Ju, Li Tian, and Kun Zhou. A posteriori error analysis of finite element method for linear nonlocal diffusion and peridynamic models. *Mathematics of Computation*, 82(284):1889–1922, 2013.

[14] Qiang Du, Li Tian, and Xuying Zhao. A convergent adaptive finite element algorithm for nonlocal diffusion and peridynamic models. *SIAM Journal on Numerical Analysis*, 51(2):1211–1234, 2013.

[15] Yalchin Efendiev and Thomas Y Hou. *Multiscale finite element methods: theory and applications*, volume 4. Springer Science & Business Media, 2009.

[16] Carlos Fiolhais, Fernando Nogueira, and Miguel AL Marques. *A primer in density functional theory*, volume 620. Springer Science & Business Media, 2003.

[17] Max Gunzburger and Richard B Lehoucq. A nonlocal vector calculus with application to nonlocal boundary value problems. *Multiscale Modeling & Simulation*, 8(5):1581–1598, 2010.

[18] Ulrich L Hetmaniuk and Richard B Lehoucq. A special finite element method based on component mode synthesis. *ESAIM: Mathematical Modelling and Numerical Analysis*, 44(03):401–420, 2010.

[19] Pierre Hohenberg and Walter Kohn. Inhomogeneous electron gas. *Physical Review*, 136(3B):B864, 1964.

[20] Walter Kohn and Lu Jeu Sham. Self-consistent equations including exchange and correlation effects. *Physical Review*, 140(4A):A1133, 1965.

[21] Richard B Lehoucq and Mark P Sears. Statistical mechanical foundation of the peridynamic nonlocal continuum theory: Energy and momentum conservation laws. *Physical Review E*, 84(3):031112, 2011.

[22] Richard B Lehoucq and Stewart A Silling. Statistical coarse-graining of molecular dynamics into peridynamics. *Report SAND2007-6410, Sandia National Laboratories, Albuquerque, New Mexico*, 2007.

[23] M. L. Parks, D. J. Littlewood, J. A. Mitchell, and S. A. Silling. Peridigm Users' Guide v1.0.0. SAND Report 2012-7800, Sandia National Laboratories, Albuquerque, NM and Livermore, CA, 2012.

[24] John P Perdew and Stefan Kurth. Density functionals for non-relativistic coulomb systems in the new century. In *A primer in density functional theory*, pages 1–55. Springer, 2003.

[25] R Rahman and JT Foster. Peridynamic theory of solids from the perspective of classical statistical mechanics. *Physica A: Statistical Mechanics and its Applications*, 2015.

[26] R Rahman and A Haque. A peridynamics formulation based hierarchical multiscale modeling approach between continuum scale and atomistic scale. *International Journal of Computational Materials Science and Engineering*, 1(03):1250029, 2012.

[27] Béatrice Rivière. *Discontinuous Galerkin methods for solving elliptic and parabolic equations: theory and implementation*. Society for Industrial and Applied Mathematics, 2008.

[28] A.G. Salinger, R.A. Bartlett, Q. Chen, X. Gao, G.A. Hansen, I. Kalashnikova, A. Mota, R.P. Muller, E. Nielsen, J.T. Ostien, R.P. Pawlowski, E.T. Phipps, and W. Sun. Albany: A component–based partial differential equation code built on trilinos. SAND Report 2013-8430J, Sandia National Laboratories, Albuquerque, NM and Livermore, CA, 2013.

[29] Pablo Seleson, Michael L Parks, Max Gunzburger, and Richard B Lehoucq. Peridynamics as an upscaling of molecular dynamics. *Multiscale Modeling & Simulation*, 8(1):204–227, 2009.

[30] Pablo D Seleson. *Peridynamic multiscale models for the mechanics of materials: constitutive relations, upscaling from atomistic systems, and interface problems*. PhD thesis, Florida State University, 2010.

[31] RE Showalter. Hilbert space methods for partial differential equations. *Electronic Monographs in Differential Equations, San Marcos, TX*, 1994.

[32] SA Silling, M Epton, O Weckner, J Xu, and E Askari. Peridynamic states and constitutive modeling. *Journal of Elasticity*, 88(2):151–184, 2007.

[33] SA Silling and RB Lehoucq. Peridynamic theory of solid mechanics. *Advances in Applied Mechanics*, 44(1):73–166, 2010.

[34] SA Silling, O Weckner, E Askari, and F Bobaru. Crack nucleation in a peridynamic solid. *International Journal of Fracture*, 162(1-2):219–227, 2010.

[35] Stewart A Silling. Reformulation of elasticity theory for discontinuities and long-range forces. *Journal of the Mechanics and Physics of Solids*, 48(1):175–209, 2000.

[36] Stewart A Silling. Linearized theory of peridynamic states. *Journal of Elasticity*, 99(1):85–111, 2010.

[37] Stewart A Silling. A coarsening method for linear peridynamics. *International Journal for Multiscale Computational Engineering*, 9(6), 2011.

[38] Stewart A Silling and James V Cox. Hierarchical Multiscale Method Development for Peridynamics. SAND Report 2014-18565, Sandia National Laboratories, Albuquerque, NM and Livermore, CA, 2014.

[39] Stewart A Silling and Richard B Lehoucq. Convergence of peridynamics to classical elasticity theory. *Journal of Elasticity*, 93(1):13–37, 2008.

[40] EB Tadmor, R Phillips, and M Ortiz. Mixed atomistic and continuum models of deformation in solids. *Langmuir*, 12(19):4529–4534, 1996.

[41] AP Thompson, LP Swiler, CR Trott, SM Foiles, and GJ Tucker. Spectral neighbor analysis method for automated generation of quantum-accurate interatomic potentials. *Journal of Computational Physics*, 285:316–330, 2015.

[42] Xiaochuan Tian and Qiang Du. Asymptotically compatible schemes and applications to robust discretization of nonlocal models. *SIAM Journal on Numerical Analysis*, 52(4):1641–1665, 2014.

[43] Xiaochuan Tian and Qiang Du. Nonconforming discontinuous galerkin methods for nonlocal variational problems. *SIAM Journal on Numerical Analysis*, 53(2):762–781, 2015.

[44] Gregory J Wagner and Wing Kam Liu. Coupling of atomistic and continuum simulations using a bridging scale decomposition. *Journal of Computational Physics*, 190(1):249–274, 2003.

DISTRIBUTION:

2 Department of Mathematics
Kidder Hall 368
Oregon State University
Corvallis, Oregon

1 MS 0845 Michael Tupek, 1542
1 MS 1318 Stephen Bond, 1442
1 MS 1318 Stan Moore, 1444
1 MS 1320 Pavel Bochev, 1442
1 MS 1320 Scott Collis, 1440
1 MS 1320 Richard Lehoucq, 1442
1 MS 1320 Michael Parks, 1442
1 MS 1320 Mauro Perego, 1442
1 MS 1321 Marta D'Elia, 1441
1 MS 1321 Veena Tikare, 1444
1 MS 1322 David Littlewood, 1444
1 MS 1322 John Mitchell, 1444
1 MS 1322 Stewart Silling, 1444
1 MS 9042 James Foulk, 8256
1 MS 9042 Jakob Ostien, 8256
1 MS 9957 Alejandro Mota, 8256
2 Timothy Costa
2 Malgorzata Peszynska
1 MS 0899 Technical Library, 9536 (electronic copy)

This page intentionally left blank.


Sandia National Laboratories